Gear Crack Propagation Path Studies— Guidelines for Ultra-Safe Design

David G. Lewicki
U.S. Army Research Laboratory, Glenn Research Center, Cleveland, Ohio

Since its founding, NASA has been dedicated to the advancement of aeronautics and space science. The NASA Scientific and Technical Information (STI) Program Office plays a key part in helping NASA maintain this important role.

The NASA STI Program Office is operated by Langley Research Center, the Lead Center for NASA's scientific and technical information. The NASA STI Program Office provides access to the NASA STI Database, the largest collection of aeronautical and space science STI in the world. The Program Office is also NASA's institutional mechanism for disseminating the results of its research and development activities. These results are published by NASA in the NASA STI Report Series, which includes the following report types:

- TECHNICAL PUBLICATION. Reports of completed research or a major significant phase of research that present the results of NASA programs and include extensive data or theoretical analysis. Includes compilations of significant scientific and technical data and information deemed to be of continuing reference value. NASA's counterpart of peer-reviewed formal professional papers but has less stringent limitations on manuscript length and extent of graphic presentations.

- TECHNICAL MEMORANDUM. Scientific and technical findings that are preliminary or of specialized interest, e.g., quick release reports, working papers, and bibliographies that contain minimal annotation. Does not contain extensive analysis.

- CONTRACTOR REPORT. Scientific and technical findings by NASA-sponsored contractors and grantees.

- CONFERENCE PUBLICATION. Collected papers from scientific and technical conferences, symposia, seminars, or other meetings sponsored or cosponsored by NASA.

- SPECIAL PUBLICATION. Scientific, technical, or historical information from NASA programs, projects, and missions, often concerned with subjects having substantial public interest.

- TECHNICAL TRANSLATION. English-language translations of foreign scientific and technical material pertinent to NASA's mission.

Specialized services that complement the STI Program Office's diverse offerings include creating custom thesauri, building customized data bases, organizing and publishing research results . . . even providing videos.

For more information about the NASA STI Program Office, see the following:

- Access the NASA STI Program Home Page at *http://www.sti.nasa.gov*

- E-mail your question via the Internet to help@sti.nasa.gov

- Fax your question to the NASA Access Help Desk at 301–621–0134

- Telephone the NASA Access Help Desk at 301–621–0390

- Write to:
  NASA Access Help Desk
  NASA Center for AeroSpace Information
  7121 Standard Drive
  Hanover, MD 21076

NASA/TM—2001-211073

ARL–TR–2468

Gear Crack Propagation Path Studies— Guidelines for Ultra-Safe Design

David G. Lewicki
U.S. Army Research Laboratory, Glenn Research Center, Cleveland, Ohio

National Aeronautics and
Space Administration

Glenn Research Center

July 2001

Available from

Gear Crack Propagation Path Studies - Guidelines for Ultra-Safe Design

David G. Lewicki
U.S. Army Research Laboratory
National Aeronautics and Space Administration
Glenn Research Center
Cleveland, Ohio
david.g.lewicki@grc.nasa.gov

Design guidelines have been established to prevent catastrophic rim fracture failure modes when considering gear tooth bending fatigue. Analysis was performed using the finite element method with principles of linear elastic fracture mechanics. Crack propagation paths were predicted for a variety of gear tooth and rim configurations. The effects of rim and web thicknesses, initial crack locations, and gear tooth geometry factors such as diametral pitch, number of teeth, pitch radius, and tooth pressure angle were considered. Design maps of tooth/rim fracture modes including effects of gear geometry, applied load, crack size, and material properties were developed. The occurrence of rim fractures significantly increased as the backup ratio (rim thickness divided by tooth height) decreased. The occurrence of rim fractures also increased as the initial crack location was moved down the root of the tooth. Increased rim and web compliance increased the occurrence of rim fractures. For gears with constant pitch radii, coarser-pitch teeth increased the occurrence of tooth fractures over rim fractures. Also, 25° pressure angle teeth had an increased occurrence of tooth fractures over rim fractures when compared to 20° pressure angle teeth. For gears with constant number of teeth or gears with constant diametral pitch, varying size had little or no effect on crack propagation paths.

Introduction

Effective gear designs balance strength, durability, reliability, size, weight, and cost. However, unexpected gear failures may occur even with adequate gear tooth design (Ref. 1). In order to design an extremely safe system, the designer must ask and address the question "what happens when a failure occurs." With regard to gear tooth bending fatigue, tooth or rim fractures may occur. For aircraft, a crack which propagates through a rim would be catastrophic, leading to disengagement of a rotor or propeller, loss of an aircraft, and possible fatalities (Refs. 2 and 3). This failure mode should be avoided. A crack which propagates through a tooth itself may or may not be catastrophic, depending on the design and operating conditions. Also, early warning of this failure mode may be possible due to advances in modern diagnostic systems (Ref. 4).

Fracture mechanics has developed into a useful discipline for predicting strength and life of cracked structures. Linear elastic fracture mechanics applied to gear teeth has become increasingly popular. Among the earliest, fracture mechanics was applied to gear teeth to simulate crack propagation, compute threshold loads, estimate stress intensity factors, and calculate tooth life (Refs. 5–7). Researchers at Tohoku University in Japan performed a series of analyses and experiments to determine the effect of residual stress on crack initiation and propagation (Refs. 8 and 9). In addition, a comprehensive, self-contained analysis package to refine the spur gear bending fatigue theory using fracture mechanics was developed (Ref. 10).

The stress intensity factors are the key parameters to estimate the characteristics of a crack. Analytical methods using weight function techniques to estimate gear tooth stress intensity factors have been developed (Refs. 11 and 12). Numerical techniques such as the finite element method and

boundary element method have also been studied (Refs. 13 and 14). Based on stress intensity factors, fatigue crack growth and gear life predictions have been investigated (Refs. 15–18). In addition, gear crack trajectory predictions have been addressed in a few studies (Refs. 19–25).

The objective of the current study is to develop design guidelines to prevent catastrophic rim fracture failure modes when considering gear tooth bending fatigue. Analysis was performed using the finite element method with principles of linear elastic fracture mechanics. Crack propagation paths were predicted for a variety of gear tooth and rim configurations. The effects of rim and web thicknesses, initial crack locations, and gear tooth geometry factors such as diametral pitch, number of teeth, pitch radius, and tooth pressure angle were considered. Crack trajectories are presented for the variety of cases studied along with design maps indicating gear tooth or gear rim fracture modes. It should be noted that the current study investigates the likelihood of tooth or rim fracture assuming an initial crack is present. The absolute probability of fracture should include crack initiation, but is beyond the scope of this work.

Gear Modeling

Basic gear tooth geometry data was input to a tooth coordinate generation computer program. The tooth coordinate generator program used the method of Ref. 26 to determine the tooth coordinates. The output was tooth coordinate and rim coordinate data which defined a single-tooth sector of a gear. This output was used by a commercially available pre- and post-processing finite element analysis software package (Ref. 27). This package created the finite element mesh of the complete gear. The mesh was then imported to the FRANC (FRacture ANalysis Code) computer program.

FRANC is a general purpose finite element code for the static analysis of cracked structures (Ref. 28). The program is designed for two-dimensional problems, uses principles of linear elastic fracture mechanics, and is capable of analyzing plane strain, plane stress, or axi-symmetric problems. Eight-node quadrilateral or six-node triangular elements can be used. Among the variety of capabilities, a unique feature of the program is the ability to model a crack in a structure. The program uses a method called "delete and fill" to accomplish this. To illustrate, consider a finite element mesh of an uncracked structure. The user would first define an initial crack by identifying the node of the crack mouth and

step), the program solves the finite element equations, calculates the stress intensity factors, and calculates the crack propagation angle. The program then places the new crack tip at the calculated angle and at a user-defined crack increment length. The model is then re-meshed using the "delete and fill" method described above. The procedure is repeated a number of times as specified by the user. Fig. 1c shows the predicted crack propagation path of a gear tooth. In this example, the predicted crack trajectory was after 29 steps, i.e., the crack trajectory was approximated by 29 line segments. In previous studies, gear crack propagation paths calculated from the FRANC computer program were validated from experimental tests (Refs. 19, 24). Such a
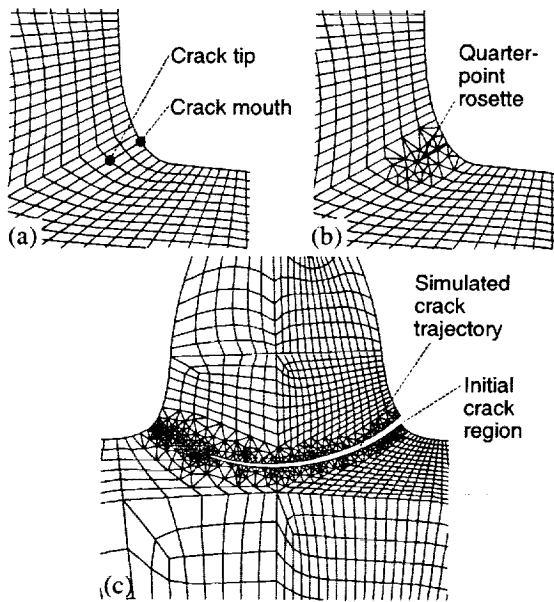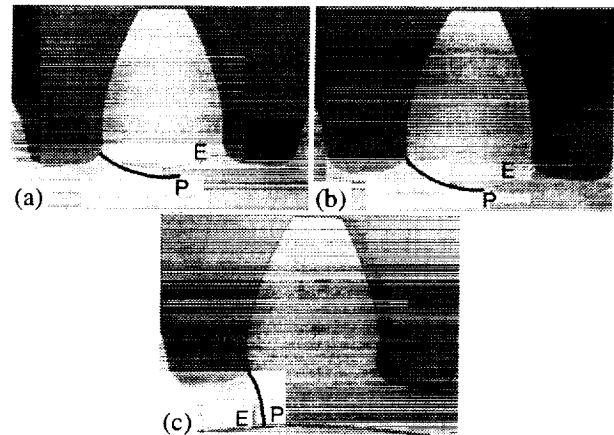

Fig. 1. Crack modeling scheme using finite element method. (a) user-defined initial crack, (b) final mesh of initial crack, (c) predicted crack propagation path.

Fig. 2. Comparison of predicted gear tooth crack propagation paths with experimental results, P=predicted, E=experiments (Ref. 24). (a) m_b=3.3, (b) m_b=1.0, (c) m_b=0.5.

coordinates of the crack tip (Fig. 1a). FRANC would then delete the elements in the vicinity of the crack tip, insert a rosette of quarter-point, six-node triangular elements around the crack tip to model the inverse square-root stress singularity, then fill the remaining area between the rosette and original mesh with conventional six-node triangular elements (Fig. 1b). The user would then run the finite element equation solver to determine nodal displacements, forces, stresses, and strains. Mode I and mode II stress intensity factors, K_I and K_{II}, respectively, can be calculated using a variety of methods. (As a refresher, mode I loading refers to loads applied normal to the crack plane which tend to open the crack. Mode II refers to in-plane shear loading.) The stress intensity factors quantify the state of stress in the region near the crack tip. In the program, the stress intensity factors can also be used to predict the crack propagation trajectory angles, again using a variety of methods.

A further unique feature of FRANC is the automatic crack propagation capability. After an initial crack is inserted in a mesh, the program simulates crack propagation as a number of straight line segments. For each segment (or

validation is shown in Fig. 2. Here, the effect of rim thickness (expressed as backup ratio, m_b, defined in the next paragraph) on crack path was explored. Notches were placed in the fillet region of the test gear teeth and run in a fatigue test rig until tooth or rim fracture occurred. The FRANC program was also used in these studies to model the gears. Initial cracks were inserted in the tooth fillets (corresponding to the notch locations of the test gears) and propagated as described above. As seen from the figure, the program was successful in predicting the crack paths.

A typical finite element gear model used in the current study is shown in Fig. 3. The mesh shown is for an uncracked gear. The gear design is the baseline used in the current study. The design parameters are: 28 teeth, 8 diametral pitch, 1.75-in pitch radius, 20° pressure angle, and a 0.25-in face width. The model had 2255 plane stress, 8-node, quadrilateral elements and 7122 nodes. For improved accuracy, the mesh was refined in the upper portion of the model (this is the region where cracks will be inserted). The tooth load was placed at the highest point of single tooth contact (HPSTC), normal to the surface. Although the tooth load changes in magnitude and direction in actual gear operations, a static analysis with the load at the HPSTC has given accurate results with respect to crack
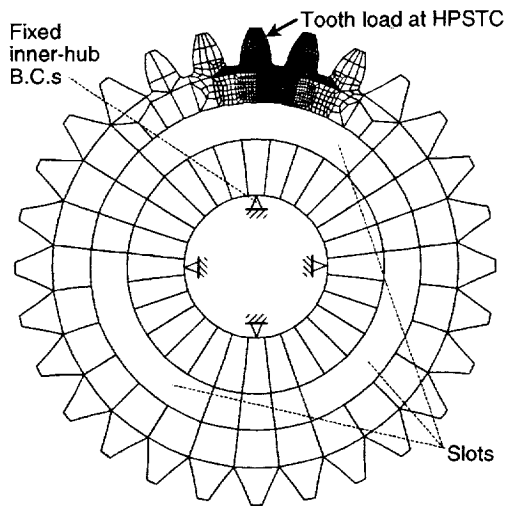
Fig. 3. Typical finite element model of an uncracked gear; 28 teeth, 8 diametral pitch, 1.75-in pitch radius, 20° pressure angle, m_b=1.0.

Fig. 4. Definition of terms. (a) backup ratio, m_b=b/h, (b) initial crack location angle, θ_0.

propagation analysis (Ref. 24). Four hub nodes at the gear inner diameter were fixed to ground for boundary conditions. The material used was steel. In addition, slots were incorporated in the model to model thin-rim gears. The model shown has a backup ratio, m_b=1.0. The backup ratio is defined as the rim thickness, b, divided by the tooth height, h (Fig. 4a). As stated before, crack propagation angles are determined from the calculated stress intensity factors. In the current study, the stress intensity factors were determined from the finite element method nodal displacements and forces using the J-integral method (Ref. 29). In addition, the crack propagation angles were determined from the stress intensity factors using the maximum tangential stress theory (Ref. 30).

Effects of Backup Ratio and Initial Crack Location on Crack Propagation

Gear models with backup ratios m_b of 0.5, 0.6, 0.7, 0.8, 0.9, 1.0, 1.1, 1.2, and 1.3 were investigated. These models were based on that shown in Fig. 3, but with various slot heights to give the appropriate rim thicknesses. Also, the effect of initial crack location, θ_0, was investigated. The location of the initial crack is defined in Fig. 4b. θ_0 defines the location of the initial crack mouth on the tooth fillet or root region with respect to the pitch radius.

The effect of initial crack location on crack propagation path is shown in Fig. 5 for a backup ratio of m_b=1.0. Initial crack lengths of 0.010 in were individually inserted and propagated in the models until the cracks reached either tooth or rim boundaries. This took from 25 to 49 steps, depending on the case, using a crack increment length of 0.010 in. For Fig. 5, the initial crack location angles varied from θ_0=68 to 120°. θ_0=88° corresponded to the root centerline between the tooth teeth (index 5 on Fig. 5). θ_0=104° corresponded to the location of the largest tensile stress for an uncracked gear of this design (index 8 on Fig. 5). Note that for θ_0=68 to 78°, rim fractures occurred. For θ_0=83 to 120°, tooth fractures occurred. The mode I and
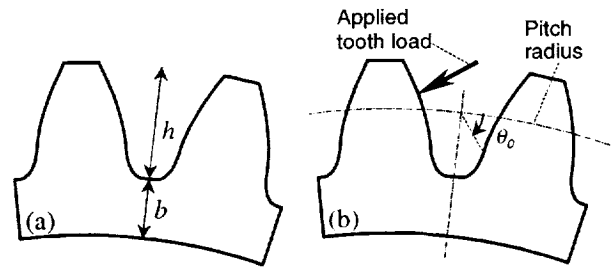
mode II stress intensity factors as a function of crack length for the m_b=1.0 gear crack models of Fig. 5 are shown in Fig. 6. These are for an applied tooth load of Q=364 lb. For clarity, not all the initial crack location cases are shown in the figure. For the rim fracture cases (θ_0=68 to 78°), only the θ_0=68 case is shown for mode I. The other rim fracture cases, however, had nearly identical responses. Also note that the K_I magnitudes for these cases were rather low. For the tooth fracture cases, the magnitude of K_I increased as the initial crack location, θ_0, increased. Also, the K_I magnitudes had a significant increase toward the later portion of the propagation. Here, the teeth were nearly fractured off. The mode II stress intensity factor for θ_0=83 is shown in Fig. 6b. Although not exactly the same, K_{II} for the other initial crack cases was in the −1 to 3 ksi√in range. The significant observation here is that the mode I stress intensity factors are much greater in magnitude than the mode II. This implies that the crack propagation paths are smooth, continuous, and, in most cases, rather straight with only a slight curvature. This matches that seen in field experience for gear
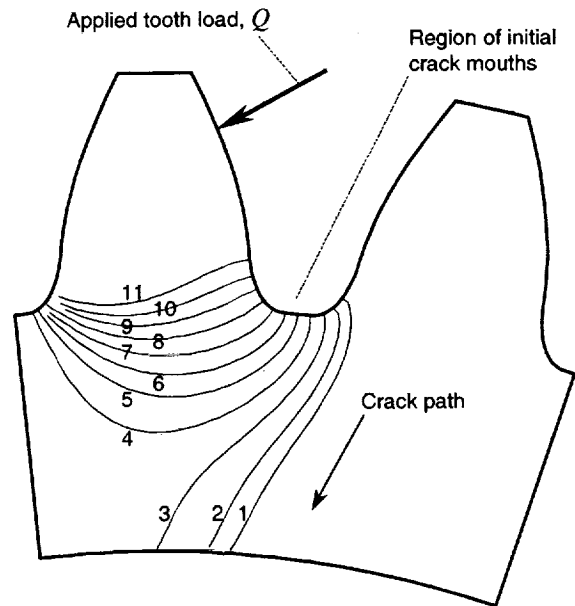

Fig. 5. Effect of initial crack location on crack propagation path, m_b=1.0, 1) θ_0=68°, 2) θ_0=73°, 3) θ_0=78°, 4) θ_0=83°, 5) θ_0=88°, 6) θ_0=94°, 7) θ_0=99°, 8) θ_0=104°, 9) θ_0=109°, 10) θ_0=114°, 11) θ_0=120°.
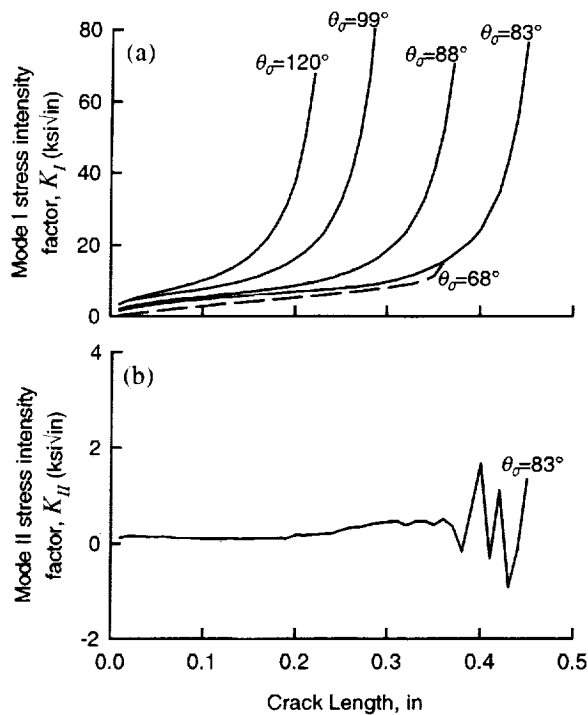
Fig. 6. Stress intensity factors from gear crack propagation studies, m_b=1.0, Q=364 lb. (a) mode I, (b) mode II.

Fig. 7. Effect of backup ratio and initial crack location on propagation path.

tooth bending fatigue. (Again, as a refresher, the magnitude of K_I determines the crack propagation rate while K_{II} determines the crack propagation direction. For K_{II}=0, the crack propagates in a straight path. For $K_{II}\neq0$ and much smaller than K_I, the crack propagates in a slightly curved path. The crack propagation angle is a function of K_{II} / K_I).

Fig. 7 shows the effect of backup ratio and initial crack location on crack propagation. For the baseline gear design parameters and a backup ratio of m_b=1.3, tooth fractures occurred for all initial crack locations (Fig. 7i). As the backup ratio decreased, the transition from tooth fractures to rim fractures occurred at a larger initial crack location angle. Thus, for thinner rims, the occurrence of a rim fracture significantly increased. Fig. 8 shows the mode I stress intensity factors for a variety of backup ratios. Fig. 8a is for an initial crack location of θ_0=104° and Fig. 8b for θ_0=88°. Again, these corresponded to the location of the largest tensile stress for an uncracked gear and the location of the root centerline, respectively. For θ_0=104°, the K_I magnitudes were nearly identical for backup ratios m_b=0.8 to 1.3. For thinner rims, the K_I magnitudes decreased as the backup ratio decreased. This was due to the increased compliance in the gear rims, which reduced the tensile stress in the tooth fillet region. Rim fracture occurred for m_b=0.5 and tooth fractures occurred for $m_b\geq0.6$ for the θ_0=104° cases. For θ_0=88° and for crack lengths less than 0.2 in, the K_I magnitudes were slightly less than those for the θ_0=104°. This occurred because the crack tip regions were located further down the fillet toward the root where the tensile stress was lower. An exception to this was the m_b=0.5 case where the K_I magnitudes were about the same for θ_0=88 and
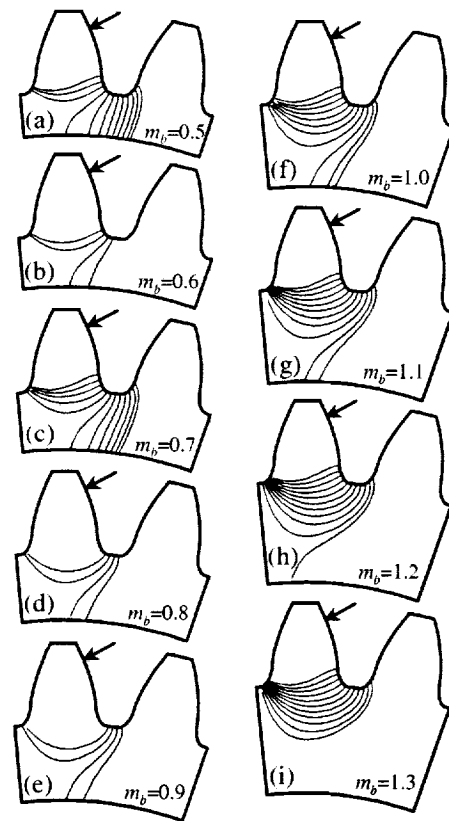
104°. For crack lengths greater than 0.2 in, larger crack lengths were required for the θ_0=88° cases compared to the θ_0=104° cases to reach final fracture. Rim fracture occurred for $m_b\leq0.7$ and tooth fractures occurred for $m_b\geq0.8$ for the θ_0=88° cases.

Fig. 9 summarizes the crack fracture mode in a design map. Here, the crack failure mode is plotted as a function of both backup ratio and initial crack location. Note that the design space is divided into three regions: 1) tooth fractures, 2) rim fractures, and 3) no crack propagation due to compression at the initial crack tip. Again, for the baseline gear design, θ_0=104° is the location of the largest tensile stress in the tooth fillet. That would be the probable location of crack initiation as long as no material defects are considered. Thus, one would want to have a backup ratio $m_b\geq0.6$ to have only tooth failures at that location. On the other hand, if the potential for crack initiation at other locations is considered, a backup ratio of $m_b\geq1.3$ should be used to minimize the probability of rim failures.

It should be noted from Figs. 6 and 8 that the mode I stress intensity factors at the start of crack propagation are rather low for lower values of θ_0. Considering this, the design map of Fig. 9 can be adjusted using the stress intensity factor threshold concept. The stress intensity factor threshold, ΔK_{th}, is largest value of the mode I stress intensity factor in which no crack propagation would occur. It is a material property and can be derived through standard fatigue crack growth tests. Table I shows the normalized mode I stress intensity factors as a function of backup ratio
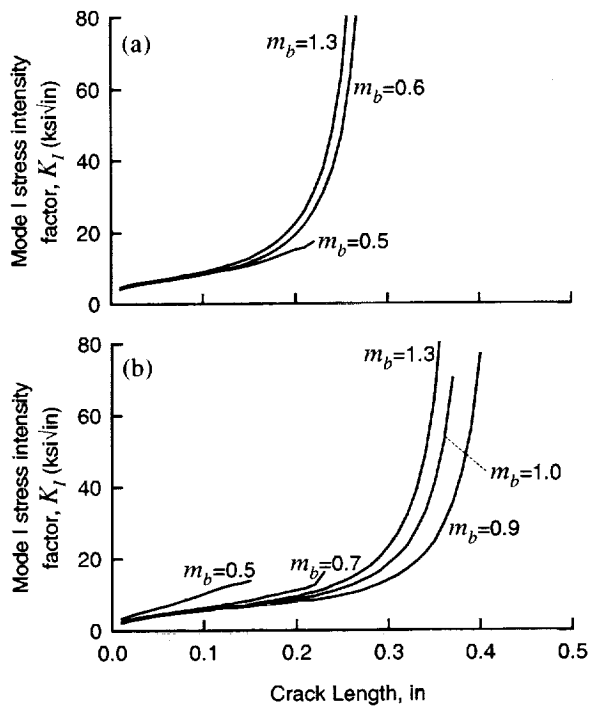
Fig. 8. Stress intensity factors from gear crack propagation studies, $Q=364$ lb (a) $\theta_0=104°$ (maximum fillet stress), (b) $\theta_0=88°$ (root centerline).
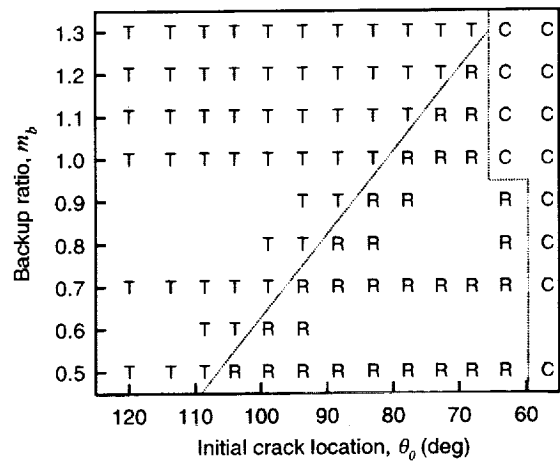

Fig. 9. Effect of backup ratio and initial crack location on crack failure modes, T=tooth fracture, R=rim fracture, C=compression (no crack propagation).
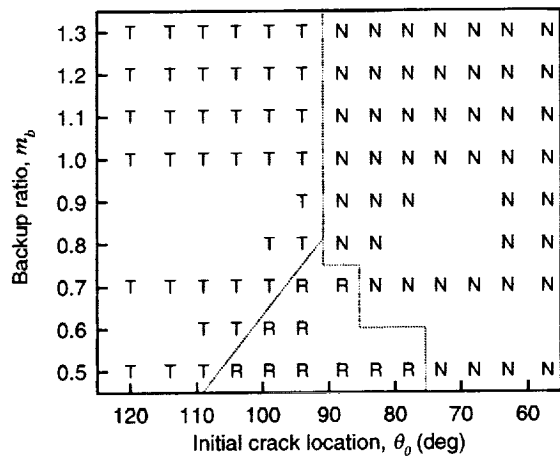

Fig. 10. Effect of backup ratio and initial crack location on crack failure modes, $Q=500$ lb, $a=0.030$ in, $\Delta K_{th}=5$ ksi√in; T=tooth fracture, R=rim fracture, N=no crack propagation.

Table I. Normalized mode I stress intensity factors, K_I/Q (in$^{-3/2}$).

(Baseline design: 28 teeth, 1.75-in pitch radius, 8-diametral pitch; crack size, $a=0.030$ in)

Backup ratio, m_B	Initial crack location, θ_0 (deg)											
	120	114	109	104	99	94	88	83	78	73	68	63
1.3	14.58	16.21	16.68	15.99	13.94	11.28	8.86	6.92	5.21	3.47	1.91	
1.2	14.54	16.12	16.55	15.85	13.80	11.17	8.79	6.91	5.24	3.54	1.99	
1.1	14.47	16.01	16.40	15.69	13.65	11.06	8.75	6.95	5.34	3.66	2.11	
1.0	14.38	15.86	16.22	15.50	13.48	10.97	8.75	7.05	5.51	3.87	2.29	
0.9						10.93	8.88	7.29	5.82			1.19
0.8					13.20	11.02	9.17	7.73				1.48
0.7	13.91	15.18	15.48	14.79	13.22	11.38	9.82	8.52	7.16	5.38	3.45	1.81
0.6			15.17	14.76	13.60	12.28						
0.5	13.30	14.49	15.00	15.11	14.84	14.29	13.33	12.22	10.62	8.14	5.30	2.98

and initial crack location for an initial crack of a=0.030 in. The normalized stress intensity factors were derived by dividing the stress intensity factors from the finite element analysis, K_I, by the applied load, Q. Since linear elastic fracture mechanics is assumed, one can scale the normalized stress intensity factors for any value of applied load, then compare the results to the stress intensity factor threshold. Fig. 10 is a modified design map as an example for an applied load of Q=500 lb, a stress intensity factor threshold ΔK_{th}=5 ksi$\sqrt{}$in (this is a typical value for AISI 9310 steel, the current standard material in aerospace drive system applications), and a crack size of a=0.030 in. For many of the cases, the mode I stress intensity factors were less than the stress intensity factor threshold, and thus, no crack propagation occurred. For the conditions of Fig. 10, a backup ratio of m_b≥0.8 should be used to ensure no rim failures will occur. This approach of using the stress intensity factor threshold concept is probably the most realistic, since cracks initiating at low θ_0 conditions are rather rare in field experience. However, the design map becomes more complex since it is dependent on gear geometry, applied load, crack size, and material properties.

Effect of Fillet Geometry on Crack Propagation

Fig. 11 shows the same basic gear tooth shape with two different fillet designs. The first is a standard fillet (Fig. 11a). The second is an increased fillet (Fig. 11b), which was used as the baseline design in the previous section. The standard fillet was derived by increasing the number of teeth of the cutting tool in the gear tooth generation process (Ref. 26). Fig. 12 shows the design map for the effect of tooth fillet on crack propagation. The increased fillet slightly increased the proportion of tooth fractures over rim fractures. Although not shown, the increased fillet had an additional benefit of reducing tensile stress in an uncracked gear.

Effect of Rim/Web Compliance on Crack Propagation

To first investigate rim compliance effects, a partial finite element model of the baseline design was developed (Fig. 13). The model was a four-tooth partial model of the baseline design (28 teeth, 8 diametral pitch, 1.75-in pitch radius, 20° pressure angle) for a backup ratio of m_b=0.9. The standard fillet design was used (Fig. 11a). The edge of the rim as well as the inner radius were fixed to ground for boundary conditions. Although m_b=0.9 is not considered a thick-rimmed gear, the boundary conditions used tended to make the rim extremely non-compliant. The tooth load was placed at the HPSTC, normal to the surface. Fig. 14 compares the crack propagation paths of the baseline slotted gear (Fig. 3, but for m_b=0.9 and with the standard fillet) to the partial-model gear of Fig. 13. The partial model gear had tooth fractures for both θ_0=83 and 88° while the slotted gear had a rim fracture for θ_0=88°. The conclusion reached was that increased rim compliance (such as with thin-rimmed gears) leads to more rim fractures.

To investigate web compliance effects, a full, non-slotted finite element model of the baseline design was developed (Fig. 15). The model had 28 teeth, 8 diametral
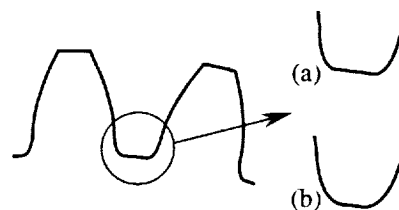

Fig. 11. Gear tooth shapes, 8 pitch, 28 teeth, pitch radius r_p=1.75 in. (a) standard fillet, (b) increased fillet.
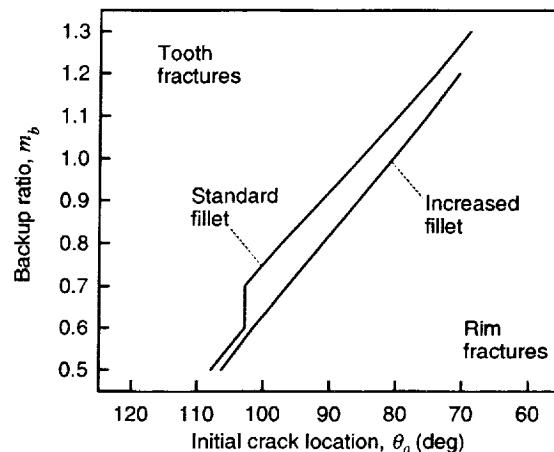

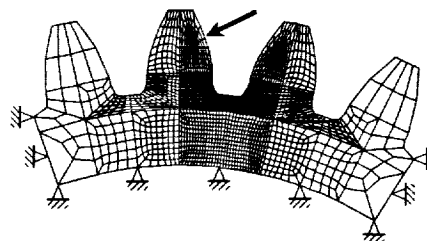**Fig. 12.** Effect of tooth fillet on crack failure modes.

Fig. 13. Finite element model for rim compliance effect on crack propagation; 28 teeth, 8 diametral pitch, 1.75-in pitch radius, 20° pressure angle, m_b=0.9.
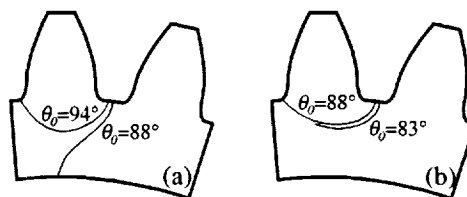

Fig. 14. Effect of rim compliance on crack propagation, m_b=1.3. (a) slotted gear, (b) partial-model gear.
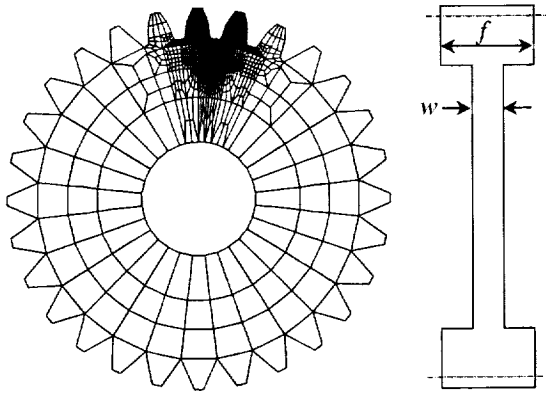
Fig. 15. Finite element model for study of rim/web compliance on crack propagation; 28 teeth, 8 diametral pitch, 1.75-in pitch radius, 20° pressure angle.

Table II. Tooth/rim deflections of uncracked gear (in).
(Design: 28 teeth, 1.75-in pitch radius, 8-diametral pitch)

Backup ratio, m_B		Slotted gear	Web thickness w=0.1 in	w=0.01 in
1.3	Tooth	0.000472	0.000780	0.005527
	Rim	0.000279	0.000506	0.004494
1.0	Tooth	0.000568	0.000794	0.005671
	Rim	0.000375	0.000536	0.004732
0.5	Tooth	0.001090	0.000834	0.005984
	Rim	0.000849	0.000598	0.005134

pitch, 1.75-in pitch radius, 20° pressure angle, and the standard fillet design. A plane stress, two-dimensional approximation was still used, but different thicknesses were specified for the tooth/rim face width, f, and the web thickness, w. Two different web thicknesses (w=0.1 and 0.01 in) were studied and compared to the slotted baseline design. For all cases, the tooth face width was f=0.25 in. As before, a tooth load of Q=364 lb was placed at the HPSTC, normal to the surface, and four hub nodes at the gear inner diameter were fixed to ground for boundary conditions. Table II gives the loaded tooth and rim deflections for an uncracked gear. Fig. 16 shows the effect of web thickness on crack propagation. Three backup ratios, m_b=1.3, 1.0, and 0.5, were studied.

For m_b=1.3, the w=0.1-in model was slightly more compliant than the slotted model (Table II). However, tooth fractures occurred for all cases of initial crack location $62°\le\theta_0\le119°$ for the w=0.1-in model (Fig. 16b) while rim fractures occurred in the slotted model for $\theta_0\le67°$ (Fig. 16a). This was also the trend for the m_b=1.0 case except rim fractures occurred in the slotted model for $\theta_0\le83°$ (Fig. 16d). For both m_b=1.3 and 1.0 and the w=0.01-in model, the compliance was significantly increased (Table II) and rim fractures occurred for $\theta_0\le77°$ (Fig. 16c) and $\theta_0\le88°$ (Fig. 16f), respectively. For m_b=0.5, the slotted model and the w=0.01-in model produced rim fractures for $\theta_0\le106°$
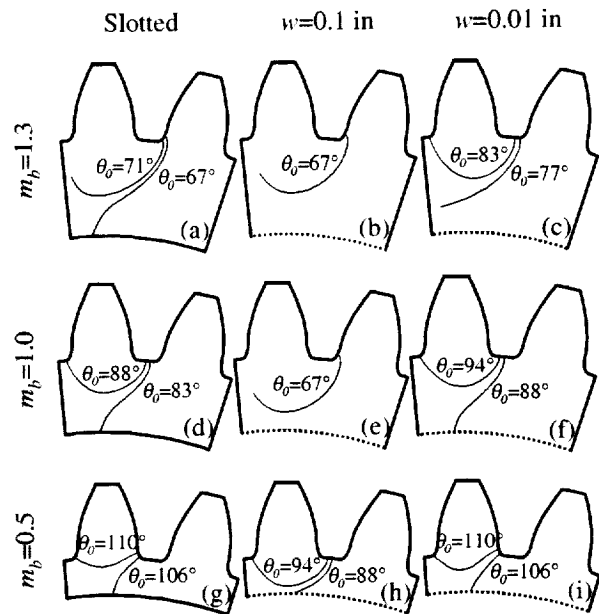

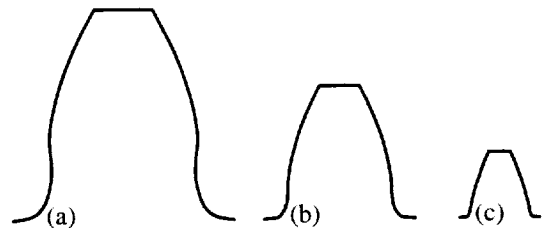**Fig. 16.** Effect of web thickness on crack propagation.

Fig. 17. Gear tooth shapes, pitch radius, r_p=1.75 in.
(a) 5.142857 pitch, 18 teeth, (b) 8 pitch, 28 teeth,
(c) 16 pitch, 56 teeth.

(Figs. 16g, 16i). The conclusion reached was that increased web compliance also lead to more rim fractures. However, when comparing a slotted gear to a webbed gear, compliance was not the only factor in determining tooth/rim fracture transition conditions.

Effect of Gear Size on Crack Propagation

The basic size of a tooth is determined by the fundamental equation:

$$P = \frac{N}{2\, r_p}$$

where P is the diametral pitch (in^{-1}), N is the number of teeth, and r_p is the pitch radius (in). Three different schemes were used in determining size effects on crack propagation: 1) constant pitch radius, 2) constant number of teeth, and 3) constant diametral pitch.

Constant pitch radius. Fig. 17 shows three different tooth shapes for a constant pitch radius of r_p=1.75 in: a) 5.142857 diametral pitch, 18 teeth, b) 8 pitch, 28 teeth, and c) 16 pitch, 56 teeth. Case (b) was the baseline model described previously. Models for cases (a) and (c) are shown
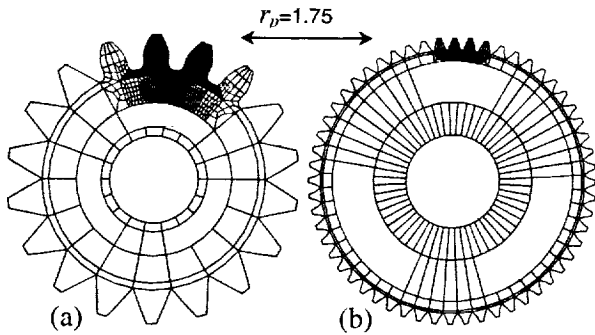
Fig. 18. Finite element models for gear size effect studies on crack propagation. (a) 5.142857 pitch, 18 teeth, (b) 16 pitch, 56 teeth.
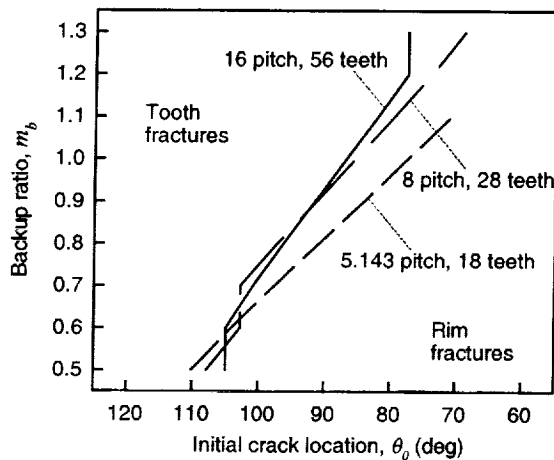

Fig. 19. Effect of pitch and number of teeth on crack failure modes (constant pitch radius, r_p=1.75 in).

Fig. 20. Simple machine elements. (a) cantilever beam in bending, (b) axially loaded bar.

Fig. 21. Gear tooth shapes, 8 pitch. (a) 28 teeth, r_p=1.75 in, (b) 56 teeth, r_p=3.50 in, (c) 84 teeth, r_p=5.25 in.

in Fig. 18. Case (a) had 2226 elements and 6973 nodes while case (c) had 2396 elements and 7675 nodes. As before, the tooth load was placed at the HPSTC, normal to the surface, and four hub nodes at the gear inner diameter were fixed to ground for boundary conditions. Fig. 19 shows the design map (backup ratio and initial crack location effects on tooth or rim fractures) for the three cases. The 8-pitch, 28-tooth, model and the 16-pitch, 56-tooth model had nearly identical responses. The 5.142857-pitch, 18-tooth model had increased tooth-fracture conditions, indicating a decreased rim compliance condition.

Constant number of teeth. Keeping the number of teeth constant and varying the size by proportionally varying the diametral pitch and pitch radius has the effect of scaling the design geometrically. That is, a design with N=56 teeth, P=8 (in^{-1}) diametral pitch, and r_p=3.50 in is geometrically twice as big as a design with N=56, P=16 (in^{-1}), and r_p=1.75 in. Similarly, a N=56, P=5.283 (in^{-1}), and r_p=5.25 in is three times as big. To investigate this size effect on crack propagation, consider two simple machine elements: 1) cantilever beam in bending, and 2) axially loaded bar (Fig. 20). A gear tooth can be roughly approximated by a cantilever beam in bending and an axially loaded bar in
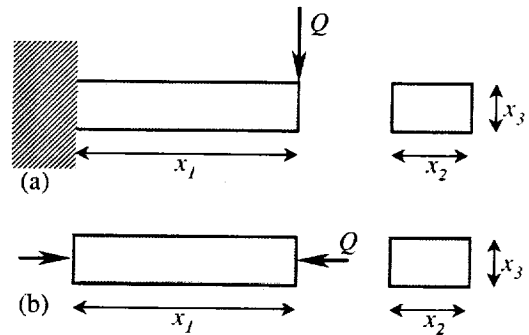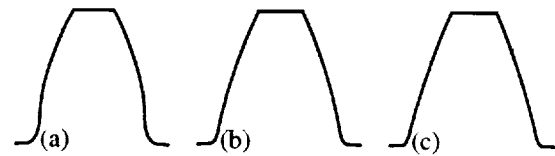
compression due to the tangential and radial tooth loads. The deflection, δ, and stress, σ, of a cantilever beam in bending with a rectangular cross section are:

$$\delta = \frac{4Qx_1^3}{Ex_2x_3^3}, \quad \sigma = \frac{6Qx_1}{x_2x_3^2}$$

where E is Young's modulus. The deflection and stress of an axial bar in compression with a rectangular cross section are:

$$\delta = \frac{Qx_1}{Ex_2x_3}, \quad \sigma = \frac{Q}{x_2x_3}$$

For both bending and compression, if the size is doubled, the magnitudes of the deflections are one-half of those for the original size for the same applied load and material as long as linear elastic conditions are applicable. Also, if the size is doubled, the magnitudes of the stresses are one-fourth of those for the original size. This proportioning is also applicable to the stress intensity factors, assuming linear elastic fracture mechanics. Recall that the crack propagation angles are a function of K_{II} / K_I. Since K_I and K_{II} are proportioned identically from the size effect, the ratio K_{II} / K_I remains the same. Therefore, the crack propagation paths are same. Thus, keeping a constant number of teeth and varying the diametral pitch and pitch radius has no effect on the crack propagation path. As a note, these results were validated using finite element models and procedures described in the current study.

Constant diametral pitch. Fig. 21 shows three different tooth shapes for a constant diametral pitch of P=8 in^{-1}: a) 28 teeth, r_p=1.75 in, b) 56 teeth, r_p=3.50 in, and c) 84 teeth, r_p=5.25 in. Case (a) was the baseline model described previously. The model for case (b) was the same as in Fig. 18b considering the size effect of the previous section.

A model for case (c) was developed with 2448 elements and 7969 nodes. Again, the tooth load was placed at the HPSTC, normal to the surface, and four hub nodes at the gear inner diameter were fixed to ground for boundary conditions. Fig. 22 shows the design map (backup ratio and initial crack location effects on tooth or rim fractures) for the three cases. The three cases had nearly the same response. Since the diametral pitch was identical, the basic tooth size (and thus rim size) was identical. Thus, the crack propagation paths were nearly the same.

Effect of Pressure Angle on Crack Propagation

A 20° pressure angle tooth and a 25° pressure angle tooth are depicted in Fig. 23. These were both for a 28-tooth, $P=8$ diametral pitch, $r_p=1.75$ in pitch radius design. Also, they had the same circular tooth thickness at the pitch point of $\pi/2P=0.196$ in. The 25° pressure angle tooth is wider at the base and narrower at the tip compared to the 20° pressure angle tooth. The design map for these cases is shown in Fig. 24. As seen, the 25° pressure angle tooth had increased tooth-fracture conditions, indicating a decreased rim compliance condition.
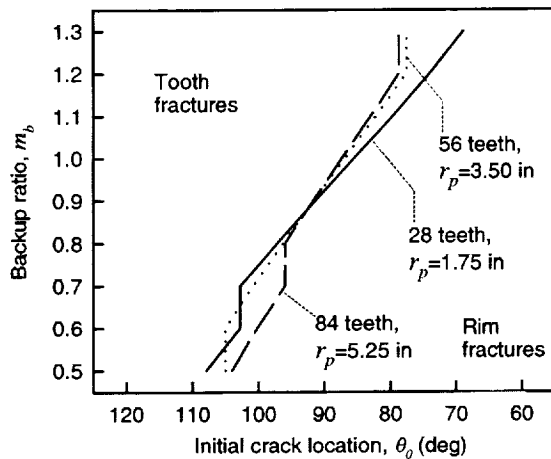

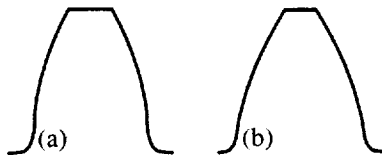**Fig. 22.** Effect of pitch radius and number of teeth on crack failure modes (constant 8-pitch gear).

Fig. 23. Gear tooth shapes, 8 pitch, 28 teeth, pitch radius, $r_p=1.75$ in. (a) 20° pressure angle, (b) 25° pressure angle.
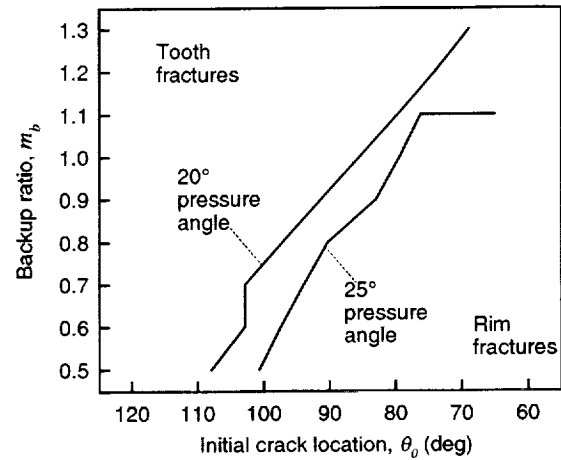

Fig. 24. Effect of pressure angle on crack failure modes.

Conclusions

Design guidelines have been established to prevent catastrophic rim fracture failure modes when considering gear tooth bending fatigue. Analysis was performed using the finite element method with principles of linear elastic fracture mechanics. Crack propagation paths were predicted for a variety of gear tooth and rim configurations. The effects of rim and web thicknesses, initial crack locations, and gear tooth geometry factors such as diametral pitch, number of teeth, pitch radius, and tooth pressure angle were considered. The following conclusions were made:

1) The occurrence of rim fractures significantly increased as the backup ratio (and thus, rim thickness) decreased. The occurrence of rim fractures also increased as the initial crack location was moved down the root of the tooth. A realistic design map of tooth/rim fracture modes included gear geometry, applied load, crack size, and material properties.

2) Increased rim compliance increased the occurrence of rim fractures. Increased web compliance also increased the occurrence of rim fractures. When comparing slotted gears to web gears, however, compliance was not the only factor in determining tooth/rim fracture transition conditions.

3) For gears with constant pitch radii, coarser-pitch teeth increased the occurrence of tooth fractures over rim fractures. Also, 25° pressure angle teeth increased the occurrence of tooth fractures over rim fractures when compared to 20° pressure angle teeth. For gears with constant number of teeth or gears with constant diametral pitch, varying size had little or no effect on crack propagation paths.

References

[1]Couchan, D.C., Barnes, G.K., and Cedoz, R.W., "Shot-Peened Gear Failures Due to Operation in a Misaligned Condition," AIAA Paper No. AIAA–93–2147, June 1993.

[2]McFadden, P.D., "Analysis of the Vibration of the Input Bevel Pinion in RAN Wessex Helicopter Main Rotor Gearbox WAK143 Prior To Failure," Aeronautical Research Laboratories Report No. AR–004–049, 1985.

[3]Albrecht, C., "Transmission Design Using Finite Element Method Analysis Techniques," *Journal of American Helicopter Society*, Vol. 33, No. 2, Apr. 1988, pp 3–14.

[4]Kershner, S., Johnson, J., and Gamauf, M., "Sikorsky Support to Commercial Health and Usage Monitoring Systems (HUMS): A Summary of Forty Months of Support," Proceedings of the AHS 53rd Forum, Virginia Beach, VA, pp. 1233–1241, Apr. 1997.

[5]Ahmad, J., and Loo, F.T., "On the Use of Strain Energy Density Fracture Criterion in the Design of Gears Using Finite Element Method," ASME Paper No. 77–DET–158, presented at the Design Technical Conference, Chicago, IL, June 1977.

[6]Honda, H., and Conway, J.C., "An Analysis by Finite Element Techniques of the Effects of a Crack in the Gear Tooth Fillet and its Applicability to Evaluating Strength of the Flawed Gears," *Bulletin of the JSME*, Vol. 22, No. 174, Dec. 1979, pp. 1848–1855.

[7]Flasker, J., and Jezernik, A., "The Comparative Analysis of Crack Propagation in the Gear Tooth," Proceedings of the International Conference of Application of Fracture Mechanics to Materials and Structures, Freiburg, West Germany, June 1983, pp. 971–982.

[8]Kato, M., Inoue, K., Deng, G., and Jeong, B.S., "Strength Evaluation of Carburized Gear Teeth Based on Fracture Mechanics," Proceedings of the KSME/JSME Joint Conference "Fracture and Strength '90," Seoul, Korea, 1990, pp. 248–253.

[9]Inoue, K., Kato, M., Deng, G., and Takatsu, N., "Fracture Mechanics Based Evaluation of Strength of Carburized Gear Teeth," Proceedings of the JSME International Conference on Motion and Power Transmissions, Hiroshima, Japan, Nov. 1991, pp. 801–806.

[10]Daniewicz, S.R., Collins, J.A., and Houser, D.R., "The Stress Intensity Factor and Stiffness for a Cracked Spur Gear Tooth," *Journal of Mechanical Design*, Vol. 116, No. 3, 1994, pp. 697–700.

[11]Nicoletto, G., "Approximate Stress Intensity Factors for Cracked Gear Teeth," *Engineering Fracture Mechanics*, Vol. 44, No. 2, 1993, pp. 231–242.

[12]Abersek, B., and Flasker, J., "Stress Intensity Factor for Cracked Gear Tooth," *Theoretical and Applied Fracture Mechanics*, Vol. 20, No. 2, 1994, pp. 99–104.

[13]Inoue, K., and Kato, M., "Crack Growth Resistance Due to Shot Peening in Carburized Gears," Presented at the 30th AIAA/ASME/SAE/ASEE Joint Propulsion Conference, Indianapolis, IN, 1994.

[14]Sfakiotakis, V.G., Katsareas, D.E., and Anifantis, N.K., "Boundary Element Analysis of Gear Teeth Fracture," *Engineering Analysis with Boundary Elements*, Vol. 20, No. 2, 1997, pp. 169–175.

[15]Blarasin, A., Guagliano, and M., Vergani, L., "Fatigue Crack Growth Predictions in Specimens Similar to Spur Gear Teeth," *Fatigue & Fracture of Engineering Materials & Structures*, Vol. 20, No. 8, 1997, pp. 1171–1182.

[16]Glodez, S., Pehan, S., and Flasker, J., "Experimental Results of the Fatigue Crack Growth in a Gear Tooth Root," *International Journal of Fatigue*, Vol. 20, No. 9, 1998, pp. 669–675.

[17]Arikin, M.A., Tarhan, A.I., and Yahoj, O.S., "Life Estimate of a Spur Gear with a Tooth Cracked at Fillet Region," Proceedings of the ASME Design Engineering Technical Conference, Atlanta, GA, 1998.

[18]Abersek, B., and Flasker, J., "Experimental Analysis of Propagation of Fatigue Crack on Gears," *Experimental Mechanics*, Vol. 38, No. 3, 1998, pp. 226–230.

[19]Lewicki, D.G., and Ballarini, R., "Effect of Rim Thickness on Gear Crack Propagation Path," *Journal of Mechanical Design*, Vol. 119, No. 1, 1997, pp. 88–95.

[20]Pehan, S., Hellen, T.K., Flasker, J., and Glodez, S., "Numerical Methods for Determining Stress Intensity Factors vs. Crack Depth in Gear Tooth Roots," *International Journal of Fatigue*, Vol. 19, No. 10, 1997, pp. 677–685.

[21]Curtin, T.J., Adey, R.A., Baynham, J.M.W., and Marais, P., "Fatigue Crack Growth Simulation for Complex Three-Dimensional Geometry and Loaded," Proceedings from the 2nd Joint NASA/FAA/DoD Conference on Aging Aircraft, Williamsburg, VA, 1998.

[22]Lewicki, D.G., Sane, A.D., Drago, R.J., and Wawrzynek, P.A., "Three-Dimensional Gear Crack Propagation Studies," Proceedings of the 4th World Congress on Gearing and Power Transmission, Paris, France, Vol. 3, 1999, pp. 2311–2324.

[23]Ciavarella, M., and Demelio, G., "Numerical Methods for the Optimization of Specific Sliding, Stress Concentration, and Fatigue Life of Gears," International Journal of Fatigue, Vol. 21, No. 5, 1999, pp. 465–474.

[24]Lewicki, D.G., Spievak, L.E., Wawrzynek, P.A., Ingraffea, A.R., and Handschuh, R.F., "Consideration of Moving Tooth Load in Gear Crack Propagation Predictions," Proceedings of the 8th International Power Transmission and Gearing Conference, Baltimore, MD, Sep. 2000.

[25]Spievak, L.E., Wawrzynek, P.A., Ingraffea, A.R., and Lewicki, D.G., "Simulating Fatigue Crack Growth in Spiral Bevel Gears," *Engineering Fracture Mechanics*, Vol. 68, No. 1, 2001, pp. 53–76.

[26]Hefeng, B., Savage, M., and Knorr, R.J., "Computer Modeling of Rack-Generated Spur Gears," *Mechanism and Machine Theory*, Vol. 20, No. 4, 1985, pp. 351–360.

[27]P3/PATRAN, P3/PATRAN User Manual, PDA Engineering, Costa Mesa, CA, 1993.

[28]Wawrzynek, P.A., "Discrete Modeling of Crack Propagation: Theoretical Aspects and Implementation Issues in Two and Three Dimensions," Ph.D. Dissertation, Cornell University, 1991.

[29]Rice, J.R., "A Path Independent Integral and the Approximate Analysis of Strain Concentration by Notches and Cracks," *Journal of Applied Mechanics*, Vol. 35, 1968, pp. 379–386.

[30]Erdogan, F., and Sih, G.C., "On the Crack Extension in Plates Under Plane Loading and Transverse Shear," *Journal of Basic Engineering*, Vol. 85, 1963, pp. 519–527.

REPORT DOCUMENTATION PAGE

Public reporting burden for this collection of information is estimated to average 1 hour per response, including the time for reviewing instructions, searching existing data sources, gathering and maintaining the data needed, and completing and reviewing the collection of information. Send comments regarding this burden estimate or any other aspect of this collection of information, including suggestions for reducing this burden, to Washington Headquarters Services, Directorate for Information Operations and Reports, 1215 Jefferson Davis Highway, Suite 1204, Arlington, VA 22202-4302, and to the Office of Management and Budget, Paperwork Reduction Project (0704-0188), Washington, DC 20503.

1. AGENCY USE ONLY (Leave blank)	2. REPORT DATE	3. REPORT TYPE AND DATES COVERED
	July 2001	Technical Memorandum

4. TITLE AND SUBTITLE

Gear Crack Propagation Path Studies—Guidelines for Ultra-Safe Design

6. AUTHOR(S)

David G. Lewicki

5. FUNDING NUMBERS

WU–712–30–13–00
1L162211A47A

7. PERFORMING ORGANIZATION NAME(S) AND ADDRESS(ES)

National Aeronautics and Space Administration
John H. Glenn Research Center
Cleveland, Ohio 44135–3191
and
U.S. Army Research Laboratory
Cleveland, Ohio 44135–3191

8. PERFORMING ORGANIZATION REPORT NUMBER

E–12912

9. SPONSORING/MONITORING AGENCY NAME(S) AND ADDRESS(ES)

National Aeronautics and Space Administration
Washington, DC 20546–0001
and
U.S. Army Research Laboratory
Adelphi, Maryland 20783–1145

10. SPONSORING/MONITORING AGENCY REPORT NUMBER

NASA TM—2001-211073
ARL–TR–2468

11. SUPPLEMENTARY NOTES

Prepared for the 57th Annual Forum and Technology Display sponsored by the American Helicopter Society, Washington, DC, May 9–11, 2001. Responsible person, David G. Lewicki, organization code 5950, 216–433–3970.

12a. DISTRIBUTION/AVAILABILITY STATEMENT

Unclassified - Unlimited
Subject Category: 37   Distribution: Nonstandard

Available electronically at http://gltrs.grc.nasa.gov/GLTRS

This publication is available from the NASA Center for AeroSpace Information, 301–621–0390.

12b. DISTRIBUTION CODE

13. ABSTRACT (Maximum 200 words)

Design guidelines have been established to prevent catastrophic rim fracture failure modes when considering gear tooth bending fatigue. Analysis was performed using the finite element method with principles of linear elastic fracture mechanics. Crack propagation paths were predicted for a variety of gear tooth and rim configurations. The effects of rim and web thicknesses, initial crack locations, and gear tooth geometry factors such as diametral pitch, number of teeth, pitch radius, and tooth pressure angle were considered. Design maps of tooth/rim fracture modes including effects of gear geometry, applied load, crack size, and material properties were developed. The occurrence of rim fractures significantly increased as the backup ratio (rim thickness divided by tooth height) decreased. The occurrence of rim fractures also increased as the initial crack location was moved down the root of the tooth. Increased rim and web compliance increased the occurrence of rim fractures. For gears with constant pitch radii, coarser-pitch teeth increased the occurrence of tooth fractures over rim fractures. Also, 25° pressure angle teeth had an increased occurrence of tooth fractures over rim fractures when compared to 20° pressure angle teeth. For gears with constant number of teeth or gears with constant diametral pitch, varying size had little or no effect on crack propagation paths.

14. SUBJECT TERMS

Gears; Crack propagation; Fracture mechanics; Finite element method; Design

15. NUMBER OF PAGES

16

16. PRICE CODE

17. SECURITY CLASSIFICATION OF REPORT	18. SECURITY CLASSIFICATION OF THIS PAGE	19. SECURITY CLASSIFICATION OF ABSTRACT	20. LIMITATION OF ABSTRACT
Unclassified	Unclassified	Unclassified	